Exclusive $B \to \pi \ell^+ \ell^-$ and $B \to \rho \, \ell^+ \ell^-$ decays in two Higgs doublet model

T. M. Aliev [*], M. Savcı [†]

Physics Department, Middle East Technical University

06531 Ankara, Turkey

Abstract

We investigate the exclusive $B \to \pi \ell^+ \ell^-$ and $B \to \rho \, \ell^+ \ell^-$ decays in framework of the general two Higgs doublet model (model III), in which an extra phase angle in the charged–Higgs fermion coupling, i.e., a new source for CP violation exists. The CP violation for both decays are calculated and it is observed that the CP violating asymmetry in model III differs significantly than the one predicted by the standard model and model II which is a special case of model III. Furthermore, it is shown that the zero value of forward backward asymmetry A_{FB} is shifted when compared with the SM value, which can also serve as the efficiency tool for establishing new physics.

PACS numbers: 12.60.–i, 13.20.–v, 13.25.Gv

[*]e-mail: taliev@rorqual.cc.metu.edu.tr

[†]e-mail: savci@rorqual.cc.metu.edu.tr

1 Introduction

Rare B meson decays, induced by flavor–changing neutral current (FCNC) $b \to s(d)$ transitions, is one of the most promising research area in particle physics. Theoretical interest to the B meson decays lies in their role as a potential precision testing ground for the standard model (SM) at loop level. Experimentally, these decays will provide quantitative information about the Cabibbo–Kobayashi–Maskawa (CKM) elements V_{td}, V_{ts} and V_{tb}. Besides these rare decay have the potential for establishing new physics beyond SM, such as two Higgs doublet model (2HDM), minimal supersymmetric extension of the SM (MSSM) [1].

Firstly the most reliable quantitative test of FCNC processes in B decays is expected to be measured in inclusive channels. In particular, the decays $B \to X_{s,d}\ell^+\ell^-$ are important probes of the effective Hamiltonian governing the FCNC transition $b \to s(d)\ell^+\ell^-$. The hope that $B \to X_s\ell^+\ell^-$ decay will be measurable in experiments in the near future, encourage extensive investigation of this process in the SM, 2HDM and MSSM [2]–[15]. The matrix element of the $b \to s\ell^+\ell^-$ contains terms describing the virtual effects induced by $t\bar{t}$, $c\bar{c}$ and $u\bar{u}$ loops which are proportional to $V_{tb}V_{ts}^*$, $V_{bc}V_{cs}^*$ and $V_{bu}V_{su}^*$, respectively. Using unitarity of the CKM matrix and neglecting $V_{bu}V_{su}^*$ in comparison to $V_{tb}V_{ts}^*$ and $V_{bc}V_{cs}^*$, it is obvious that the matrix element for the $b \to s\ell^+\ell^-$ involves only one independent CKM factor $V_{tb}V_{ts}^*$ so that CP–violation in this channel is strongly suppressed in the SM.

The situation is totally different for the $b \to d\ell^+\ell^-$ decay, since all three CKM factors $V_{tb}V_{td}^*$, $V_{cb}V_{cd}^*$ and $V_{ub}V_{ud}^*$, are all of the same order (in SM) and therefore can induce considerable CP–violating difference between the decay rates of the reactions $b \to d\ell^+\ell^-$ and $\bar{b} \to \bar{d}\ell^+\ell^-$.

It should be noted here that in presence of a much stronger decay $b \to s\ell^+\ell^-$, the detection of the $b \to d\ell^+\ell^-$ decay seems to be more problematic. For this reason, in search of CP violation the corresponding exclusive decay channels $B \to \pi\ell^+\ell^-$ and $B \to \rho\,\ell^+\ell^-$ are more preferable. In general, the inclusive decays are rather difficult to measure in comparison to the exclusive ones. CP–violating effects in inclusive $b \to d\ell^+\ell^-$ and exclusive $B \to \pi\ell^+\ell^-$, $B \to \rho\,\ell^+\ell^-$ channels were studied within the framework of the SM in [15, 16].

The aim of the present work is to derive quantitative predictions for the CP violation in the exclusive $B \to \pi\ell^+\ell^-$ and $B \to \rho\,\ell^+\ell^-$ decays, in context of the general two Higgs doublet model, in which a new source for CP violation is present (see below). 2HDM model is one of the simplest extension of the SM, which contains two complex Higgs doublets, while the SM contains only one. In general, in 2HDM the flavor changing neutral currents (FCNC) that appear at tree level, are avoided by imposing an *ad hoc* discrete symmetry [18]. One possible approach to avoid these unwanted FCNC at tree level is to couple all fermions to only one of the above–mentioned Higgs doublets (model I). The other possibility is the coupling of the up and down quarks to the first and second Higgs doublets, with the vacuum expectation values v_2 and v_1, respectively (model II). Model II is more attractive since its Higgs sector coincides with the ones in the supersymmetric model. In this model there exist five physical Higgs fields: neutral scalars H^0, h^0, neutral pseudoscalar A and charged Higgs bosons $H^{\pm}$. The interaction vertex of fermions with Higgs fields depends on $tan\beta = v_2/v_1$, which is the free parameter of the model. The new experimental results of CLEO and ALEPH Collaborations [19, 20] on the branching ratio $b \to s\gamma$ decay impose strict restrictions on the charged Higgs boson mass and $tan\beta$. Recently, the lower bound on these

parameters were determined from the analysis of the $b \to s\gamma$ decay, including NLO QCD corrections [21, 22]. Other indirect bound on the ratio $m_{H^\pm}/tan\beta$ come from $B \to D\tau\bar{\nu}_\tau$ decay, where $m_{H^\pm} \geq 2.2tan\beta \, GeV$ [23], and from the τ lepton decays $m_{H^\pm} \geq 1.5 \, tan\beta \, GeV$ [24]. The consequence of an analysis without discrete symmetry has been investigated in a more general model in 2HDM, namely, model III [25, 26]. In this model FCNC appears naturally at tree level. However, the FCNC's involving the first two generations are highly suppressed, as is observed in the low energy experiments, and those involving the the third generation is not as severely suppressed as the first two generations, which are restricted by the existing experimental results.

In this work we assume that all tree level FCNC couplings are negligible. It should be noted however that, even with this assumption, the couplings of fermions to Higgs bosons may have a complex phase $e^{i\theta}$. In other words, in this model there exists a new source of CP violation that is absent in the SM, model I and model II. The effects of such an extra phase in the $b \to s\gamma$ decay were discussed in [27, 28]. The constraints on the phase angle θ in the product $\lambda_{tt}\lambda_{bb}$ of Higgs–fermion coupling (see below) imposed by the neutron electric dipole moment, $B^0 - \bar{B}^0$ mixing, ρ_0 parameter and R_b is discussed in [28].

The paper is organized as follows: In Section 2 we present the necessary theoretical framework. The branching ratios, CP–violating effects in the partial widths and forward–backward asymmetry for the above–mentioned exclusive decay channels are studied in section 3. Section 4 is devoted to the numerical analysis and concluding remarks.

2 Theoretical framework

Before presenting the necessary theoretical background, let us go through the main essential points of the general Higgs doublet model (model III). In this model, both Higgs doublets can couple to up and down quarks. Without loss of generality we can work in a basis such that the first doublet generates all the fermion and gauge boson masses, whose vacuum expectation values are

$$\langle \phi_1 \rangle = \begin{pmatrix} 0 \\ \dfrac{v}{\sqrt{2}} \end{pmatrix} \quad , \quad \langle \phi_2 \rangle \ .$$

In this basis the first doublet ϕ_1 is the same as in the SM, and all new Higgs bosons result from the second doublet ϕ_2, which can be written in the following form

$$\phi_1 = \frac{1}{\sqrt{2}} \begin{pmatrix} \sqrt{2}\, G^+ \\ v + \chi_1^0 + iG^0 \end{pmatrix} \quad , \quad \phi_2 = \frac{1}{\sqrt{2}} \begin{pmatrix} \sqrt{2}\, H^+ \\ \chi_2^0 + iA^0 \end{pmatrix} \ ,$$

where G^+ and G^0 are the Goldstone bosons. The neutral χ_1^0 and χ_2^0 are not the physical mass eigenstate, but their linear combinations give the neutral H^0 and h^0 Higgs bosons:

$$\chi_1^0 = H^0 cos\alpha - h^0 sin\alpha \ ,$$
$$\chi_2^0 = H^0 sin\alpha + h^0 cos\alpha \ .$$

The general Yukawa Lagrangian can be written as

$$\mathcal{L}_Y = \eta_{ij}^U \bar{Q}_{iL} \tilde{\phi}_1 U_{jR} + \eta_{ij}^{\mathcal{D}} \bar{Q}_{iL} \phi_1 \mathcal{D}_{jR} + \xi_{ij}^U \bar{Q}_{iL} \tilde{\phi}_2 U_{jR} + \xi_{ij}^{\mathcal{D}} \bar{Q}_{iL} \phi_2 \mathcal{D}_{jR} + h.c. \ , \tag{1}$$

where i, j are the generation indices, $\tilde{\phi} = i\sigma_2 \phi$, $\eta_{ij}^{U,\mathcal{D}}$ and $\xi_{ij}^{\mathcal{U},\mathcal{D}}$, in general, are the non–diagonal coupling matrices, $L = (1-\gamma_5)/2$ and $R = (1+\gamma_5)/2$ are the left– and right–handed projection operators. In Eq. (1) all states are weak states, that can be transformed to the mass eigenstates by rotation. After performing this rotation on the Yukawa Lagrangian, we get

$$\mathcal{L}_Y = -H^+ \bar{U} \left[V_{CKM} \hat{\xi}^{\mathcal{D}} R - \hat{\xi}^{U^+} V_{CKM} L \right] \mathcal{D} \ , \tag{2}$$

where $U(\mathcal{D})$ represents the mass eigenstates of u, c, t (d, s, b) quarks. In the present analysis, we will use a simple ansatz for $\hat{\xi}^{U^+,\mathcal{D}}$ [25],

$$\hat{\xi}^{U^+,\mathcal{D}} = \lambda_{ij} \frac{g\sqrt{m_i m_j}}{\sqrt{2} m_W} \ . \tag{3}$$

Also it assumed that λ_{ij} is complex, i.e., $\lambda_{ij} = |\lambda_{ij}| e^{i\theta}$, and for simplicity we choose $\xi^{U,\mathcal{D}}$ to be diagonal to suppress all tree level FCNC couplings, and as a result λ_{ij} are also diagonal but remain complex. Note that the results for model I and model II can be obtained from model III by the following substitutions:

$$\begin{aligned} \lambda_{tt} &= \cot\beta & \lambda_{bb} &= -\cot\beta \ \text{ for model I } , \\ \lambda_{tt} &= \cot\beta & \lambda_{bb} &= +\tan\beta \ \text{ for model II } , \end{aligned} \tag{4}$$

and $\theta = 0$.

After this brief introduction about the general Higgs doublet model, let us return our attention to the $b \to d\ell^+ \ell^-$ decay. The powerful framework into which the perturbative QCD corrections to the physical decay amplitude incorporated in a systematic way, is the effective Hamiltonian method. In this approach, the heavy degrees of freedom in the present case, i.e., t quark, $W^\pm$, $H^\pm$, h^0, H^0 are integrated out. The procedure is to match the full theory with the effective theory at high scale $\mu = m_W$, and then calculate the Wilson coefficients at lower $\mu \sim \mathcal{O}(m_b)$ using the renormalization group equations. In our calculations we choose the higher scale as $\mu = m_W$, since the charged Higgs boson is heavy enough ($m_{H^\pm} \geq 210 \ GeV$ see [21]) to neglect the evolution from $m_{H^\pm}$ to m_W.

In the version of the 2HDM we consider in this work, the charged Higgs boson exchange diagrams do not produce new operators and the operator basis is the same as the one used for the $b \to d\ell^+\ell^-$ decay in the SM. For this reason in the model under consideration, the charged Higgs boson contributions to leading order change only the value of the Wilson coefficients at m_W scale, i.e.,

$$\begin{aligned} C_7^{2HDM}(m_W) &= C_7^{SM}(m_W) + C_7^{H^\pm}(m_W) \\ C_9^{2HDM}(m_W) &= C_9^{SM}(m_W) + C_9^{H^\pm}(m_W) \\ C_{10}^{2HDM}(m_W) &= C_{10}^{SM}(m_W) + C_{10}^{H^\pm}(m_W) \ . \end{aligned}$$

The coefficients $C_i^{2HDM}(m_W)$ to the leading order are given by

$$
\begin{aligned}
C_7^{2HDM}(m_W) &= x\,\frac{(7 - 5x - 8x^2)}{24(x-1)^3} + \frac{x^2(3x-2)}{4(x-1)^4}\,\ell nx \\
&+ |\lambda_{tt}|^2\left(\frac{y(7 - 5y - 8y^2)}{72(y-1)^3} + \frac{y^2(3y-2)}{12(y-1)^4}\,\ell ny\right) \\
&+ \lambda_{tt}\lambda_{bb}\left(\frac{y(3 - 5y)}{12(y-1)^2} + \frac{y(3y-2)}{6(y-1)^3}\,\ell ny\right),
\end{aligned}
\tag{5}
$$

$$
\begin{aligned}
C_9^{2HDM}(m_W) &= -\frac{1}{sin^2\theta_W}B(m_W) + \frac{1 - 4sin^2\theta_W}{sin^2\theta_W}C(m_W) \\
&+ \frac{-19x^3 + 25x^2}{36(x-1)^3} + \frac{-3x^4 + 30x^3 - 54x^2 + 32x - 8}{18(x-1)^4}\,\ell nx + \frac{4}{9} \\
&+ |\lambda_{tt}|^2\left[\frac{1 - 4sin^2\theta_W}{sin^2\theta_W}\frac{xy}{8}\left(\frac{1}{y-1} - \frac{1}{(y-1)^2}\,\ell ny\right)\right. \\
&\left. - y\left(\frac{47y^2 - 79y + 38}{108(y-1)^3} - \frac{3y^3 - 6y^3 + 4}{18(y-1)^4}\,\ell ny\right)\right],
\end{aligned}
\tag{6}
$$

$$
\begin{aligned}
C_{10}^{2HDM}(m_W) &= \frac{1}{sin^2\theta_W}\Big(B(m_W) - C(m_W)\Big) \\
&+ |\lambda_{tt}|^2\,\frac{1}{sin^2\theta_W}\frac{xy}{8}\left(-\frac{1}{y-1} + \frac{1}{(y-1)^2}\,\ell ny\right),
\end{aligned}
\tag{7}
$$

where

$$
\begin{aligned}
B(x) &= -\frac{x}{4(x-1)} + \frac{x}{4(x-1)^2}\,\ell nx, \\
C(x) &= -\frac{x}{4}\left(\frac{x-6}{3(x-1)} + \frac{3x+2}{2(x-1)^2}\ell nx\right), \\
x &= \frac{m_t^2}{m_W^2}, \\
y &= \frac{m_{H^\pm}^2}{m_W^2}.
\end{aligned}
\tag{8}
$$

and $sin^2\theta_W = 0.23$ is the Weinberg angle. It follows from Eqs. (5–7) that among all the Wilson coefficients, only C_7 involves the new phase angle θ. We have neglected the neutral Higgs boson exchange diagram contributions, since Higgs boson–fermion interaction is proportional to the lepton mass.

The effective Hamiltonian for the $b \to d\ell^+\ell^-$ decay is [29–32]

$$
\mathcal{H} = -4\frac{G_F}{2\sqrt{2}}V_{tb}V_{td}^*\left\{\sum_{i=0}^{10}C_i(\mu)O_i(\mu) + \lambda_u\sum_{i=1}^{2}C_i(\mu)\left[O_i(\mu) - O_i^u(\mu)\right]\right\},
$$

4

where

$$\lambda_u = \frac{V_{ub}V_{ud}^*}{V_{tb}V_{td}^*} \ ,$$

and C_i are the Wilson coefficients. The explicit form of all operators O_i can be found in [29–32].

The evolution of the Wilson coefficients from the higher scale $\mu = m_W$ down to the low energy scale $\mu = m_b$ is described by the renormalization group equation

$$\mu \frac{d}{d\mu} C_i^{eff(\mu)} = C_i^{eff}(\mu)\gamma_\mu^{eff}(\mu) \ ,$$

where γ is the anomalous dimension matrix. The coefficient $C_7^{eff}(\mu)$ at the scale $\mathcal{O}(m_b)$ in NLO is calculated in [21, 22]:

$$C_7^{eff}(m_b) = C_7^0(m_b) + \frac{\alpha_s(m_b)}{4\pi} C_7^{1,eff}(m_b) \ ,$$

where $C_7^0(m_b)$ is the leading order (LO) term and $C_7^{1,eff}(m_b)$ describes the NLO terms, whose explicit forms can be found in [21]. In our case, the expressions for these coefficients can be obtained from the results of [21] by making the following replacements:

$$|Y|^2 \to |\lambda_{tt}|^2 \quad \text{and} \quad XY^* \to |\lambda_{tt}\lambda_{bb}|\, e^{i\theta} \ .$$

In the SM, the QCD corrected Wilson coefficient $C_9(m_b)$, which enters to the decay amplitude up to the next leading order has been calculated in [29–32]. The Wilson coefficient C_{10} does not receive any new corrections at all, i.e., $C_{10}(m_b) \equiv C_{10}^{2HDM}(m_W)$. As we have already noted, in the version of the 2HDM we consider in this work, there does not appear any new operator other than those that exist in the SM, therefore it is enough to make the replacement $C_9^{SM}(m_W) \to C_9^{2HDM}(m_W)$ in [29–32], in order to calculate C_9^{2HDM} at m_b scale. Hence, including the NLO QCD corrections, $C_9(m_b)$ can be written as:

$$
\begin{aligned}
C_9(\mu) = {}& C_9^{2HDM}(\mu) \left[1 + \frac{\alpha_s(\mu)}{\pi} \omega(\hat{s}) \right] \\
& + g(\hat{m}_c, \hat{s}) \left[3C_1(\mu) + C_2(\mu) + 3C_3(\mu) + C_4(\mu) + 3C_5(\mu) + C_6(\mu) \right] \\
& + \lambda_u \left[g(\hat{m}_c, \hat{s}) - g(0, \hat{s}) \right] \left(3C_1(\mu) + C_2(\mu) \right) - \frac{1}{2}g(0, \hat{s}) \left(C_3(\mu) + 3C_4(\mu) \right) \\
& - \frac{1}{2}g\left(1, \hat{s}\right)(4C_3 + 4C_4 + 3C_5 + C_6) - \frac{1}{2}g\left(0, \hat{s}\right)(C_3 + 3C_4) \\
& + \frac{2}{9}(3C_3 + C_4 + 3C_5 + C_6) \ ,
\end{aligned}
\tag{9}
$$

where $m_c = m_c/m_b$, $\hat{s} = p^2/m_b^2$, and

$$
\begin{aligned}
\omega(\hat{s}) = {}& -\frac{2}{9}\pi^2 - \frac{4}{3}Li_2(\hat{s}) - \frac{2}{3}\ell n(\hat{s})\,\ell n(1-\hat{s}) \\
& - \frac{5+4\hat{s}}{3(1+2\hat{s})}\ell n(1-\hat{s}) - \frac{2\hat{s}(1+\hat{s})(1-2\hat{s})}{3(1-\hat{s})^2(1+2\hat{s})}\ell n(\hat{s}) + \frac{5+9\hat{s}-6\hat{s}^2}{3(1-\hat{s})(1+2\hat{s})}
\end{aligned}
\tag{10}
$$

represents the $\mathcal{O}\left(\alpha_s\right)$ correction from the one gluon exchange in the matrix element of O_9, while the function $g\left(\hat{m}_c, \hat{s}\right)$ arises from one loop contributions of the four–quark operators O_1–O_6, whose form is

$$g\left(\hat{m}_c, \hat{s}\right) = -\frac{8}{9}\ell n\left(\hat{m}_i\right) + \frac{8}{27} + \frac{4}{9}y_i - \frac{2}{9}\left(2 + y_i\right)$$
$$+ \sqrt{|1 - y_i|}\left\{\Theta\left(1 - y_i\right)\left(\ell n\frac{1 + \sqrt{|1 - y_i|}}{1 - \sqrt{|1 - y_i|}} - i\pi\right) + \Theta\left(y_i - 1\right)2arctan\frac{1}{\sqrt{y_i - 1}}\right\},\ (11)$$

where $y_i = 4\hat{m}_i^2/\hat{p}^2$.

The Wilson coefficients C_9 receives also long distance contributions, which have their origin in the real $u\bar{u}$, $d\bar{d}$ and $c\bar{c}$ intermediate states, i.e., ρ, ω and J/ψ, ψ', $\cdots$. In the case of the J/ψ family this usually accomplished by introducing a Breit–Wigner distribution for the resonance through the replacement ([4–7,33])

$$g\left(\hat{m}_c, \hat{s}\right) \rightarrow g\left(\hat{m}_c, \hat{s}\right) - \frac{3\pi}{\alpha_{em}^2}\kappa \sum_{V_i = J/\psi_i, \psi', \cdots}\frac{m_{V_i}\Gamma(V_i \rightarrow \ell^+\ell^-)}{(p^2 - m_{V_i}^2) + im_{V_i}\Gamma_{V_i}}\ ,\qquad(12)$$

where the phenomenological parameter $\kappa = 2.3$ is chosen in order to reproduce correctly the experimental value of the branching ratio (see for example [16])

$$\mathcal{B}(B \rightarrow J/\psi X \rightarrow X\ell^+\ell^-) = \mathcal{B}(B \rightarrow J/\psi X)\,\mathcal{B}(J/\psi \rightarrow X\ell^+\ell^-)\ .$$

In order to avoid the double counting, in this work, as an alternative to the functions $g\left(\hat{m}_u, \hat{s}\right)$ and $g\left(\hat{m}_c, \hat{s}\right)$ that describe the effects of $u\bar{u}$ and $c\bar{c}$ loops, we have used a different procedure, in which these functions are expressed through the normalized vacuum polarization $\Pi_{had}^\gamma(\hat{s})$ that is related to the experimentally measurable quantity

$$R_{had}(\hat{s}) = \frac{\sigma_{tot}(e^+e^- \rightarrow hadrons)}{\sigma(e^+e^- \rightarrow \mu^+\mu^-)}\ ,\qquad(13)$$

via the dispersion relation (see [16, 17] for more detail). In this way it is possible to include the ρ, ω, J/ψ, ψ', $\cdots$ resonances into the differential cross section in an approximate way, consistent with the idea of global duality. In this approach the ω and J/ψ family resonances are well described through the Breit–Wigner form and ρ resonance is introduced by

$$R_{res}^\rho = \frac{1}{4}\left(1 - 4\frac{\hat{m}_\pi^2}{\hat{s}}\right)^{3/2}|F_\pi(\hat{s})|^2\ ,\qquad(14)$$

where $F_\pi(\hat{s})$ is the pion form factor that is represented by a modified Gounaris–Sakurai formula (see [34, 35]).

The effective short–distance Hamiltonian for $b \rightarrow d\ell^+\ell^-$ decay [29–32] leads to the QCD corrected matrix element (when the d quark mass is neglected)

$$\begin{aligned}\mathcal{M} &= \frac{G_F\alpha}{2\sqrt{2}\pi}V_{td}V_{tb}^*\Big\{C_9^{eff}\bar{d}\gamma_\mu(1 - \gamma_5)b\,\bar{\ell}\gamma^\mu\ell + C_{10}\bar{d}\gamma_\mu(1 - \gamma_5)b\,\bar{\ell}\gamma^\mu\gamma_5\ell\\ &- 2C_7\frac{m_b}{p^2}\bar{d}i\sigma_{\mu\nu}p^\nu(1 + \gamma_5)b\,\bar{\ell}\gamma^\mu\ell\ ,\end{aligned}\qquad(15)$$

where p^2 is the invariant dilepton mass. In Eq. (12) all Wilson coefficients are evaluated at the $\mu = m_b$ scale.

6

3 The exclusive $B \to \pi \ell^+ \ell^-$ and $B \to \rho \, \ell^+ \ell^-$ decays

In this section, we proceed to calculate the branching ratio and CP violating asymmetry in the $B \to \pi \ell^+ \ell^-$ and $B \to \rho \, \ell^+ \ell^-$ decays. It follows from the matrix element of the $b \to d \ell^+ \ell^-$ that in order to be able to calculate the matrix element of the exclusive decay $B \to M \ell^+ \ell^-$, the matrix elements $\langle M | \bar{d} \gamma_\mu (1 + \gamma_5) b | B \rangle$ and $\langle M | \bar{d} i \, \sigma_{\mu\nu} p_\nu (1 + \gamma_5) b | B \rangle$ ($M = \pi$ or ρ) have to be calculated. These matrix elements can be parametrized in the following way:

$$\left\langle \pi \left(p_\pi \right) \left| \bar{d} \gamma_\mu (1 - \gamma_5) b \right| B \left(p_B \right) \right\rangle = f^+(p^2) \left(p_B + p_\pi \right)_\mu + f^-(p^2) p_\mu , \tag{16}$$

$$\left\langle \pi \left(p_\pi \right) \left| \bar{d} i \, \sigma_{\mu\nu} p_\nu (1 + \gamma_5) b \right| B \left(p_B \right) \right\rangle = \left[\left(p_B + p_\pi \right)_\mu p^2 - p_\mu \left(m_B^2 - m_\pi^2 \right) \right] \frac{f_T(p^2)}{m_B + m_\pi} , \tag{17}$$

$$\left\langle \rho(p_\rho, \varepsilon) \left| \bar{d} \gamma_\mu (1 - \gamma_5) b \right| B \left(p_B \right) \right\rangle = -\epsilon_{\mu\nu\lambda\sigma} \varepsilon^{*\nu} p_\rho^\lambda p_B^\sigma \frac{2V(p^2)}{m_B + m_\rho}$$
$$- i \varepsilon_\mu^* (m_B + m_\rho) A_1(p^2) + i (p_B + p_\rho)_\mu (\varepsilon^* p) \frac{A_2(p^2)}{m_B + m_\rho}$$
$$+ i p_\mu (\varepsilon^* p) \frac{2 m_\rho}{p^2} \left[A_3(p^2) - A_0(p^2) \right] , \tag{18}$$

$$\left\langle \rho(p, \varepsilon) \left| \bar{d} i \sigma_{\mu\nu} p^\nu (1 + \gamma_5) b \right| B(p_B) \right\rangle = 4 \epsilon_{\mu\nu\lambda\sigma} \varepsilon^{*\nu} p^\lambda p^\sigma T_1(p^2)$$
$$+ 2i \left[\varepsilon_\mu^* (m_B^2 - m_\rho^2) - (p_B + p_\rho)_\mu (\varepsilon^* p) \right] T_2(p^2)$$
$$+ 2i (\varepsilon^* p) \left[p_\mu - (p_B + p_\rho)_\mu \frac{p^2}{m_B^2 - m_\rho^2} \right] T_3(p^2) . \tag{19}$$

In all of the matrix elements above, $p = p_B - p_M$ ($M = \pi$ or ρ) and ε^* is the four–polarization vector of the ρ meson. Using Eqs. (15–19) we obtain for the matrix elements of the $B \to \pi \ell^+ \ell^-$ and $B \to \rho \, \ell^+ \ell^-$ decays:

$$\mathcal{M}^{B \to \pi} = \frac{G \alpha}{2 \sqrt{2} \pi} V_{tb} V_{td}^* \left\{ \left(2 A p_{\pi\mu} + B p_\mu \right) \bar{\ell} \gamma_\mu \ell + \left(2 C p_{\pi\mu} + D p_\mu \right) \bar{\ell} \gamma_\mu \gamma_5 \ell \right\} , \tag{20}$$

$$\mathcal{M}^{B \to \rho} = \frac{G \alpha}{2 \sqrt{2} \pi} V_{tb} V_{td}^* \left\{ \bar{\ell} \gamma_\mu \ell \left[2 A_1 \epsilon_{\mu\nu\lambda\sigma} \varepsilon^{*\nu} p_\rho^\lambda p_B^\sigma + i B_1 \varepsilon_\mu^* - i B_2 (\varepsilon^* p)(p_B + p_\rho)_\mu - i B_3 (\varepsilon^* p) p_\mu \right] \right.$$
$$\left. + \bar{\ell} \gamma^\mu \gamma_5 \ell \left[2 C_1 \epsilon_{\mu\nu\lambda\sigma} \epsilon^{*\nu} p_\rho^\lambda p_B^\sigma + i D_1 \epsilon_\mu^* - i D_2 (\varepsilon^* p)(p_B + p_\rho)_\mu - i D_3 (\varepsilon^* p) p_\mu \right] \right\} , \tag{21}$$

where

$$A = C_9^{eff} f^+ - C_7 \frac{2 m_b f_T(p^2)}{m_B + m_\pi} ,$$
$$B = C_9^{eff} \left(f^+ + f^- \right) + C_7 \left(\frac{2 m_b f_T}{p^2} \right) \left(\frac{m_B^2 - m_\pi^2 - p^2}{m_B + m_\pi} \right) ,$$
$$C = C_{10} f^+ ,$$

$$D = C_{10}\left(f^+ + f^-\right),$$

$$A_1 = C_9^{eff}\frac{V}{m_B + m_\rho} + 4C_7\frac{m_b}{p^2}T_1,$$

$$B_1 = C_9^{eff}(m_B + m_\rho)A_1 + 4C_7\frac{m_b}{p^2}(m_B^2 - m_\rho^2)T_2,$$

$$B_2 = C_9^{eff}\frac{A_2}{m_B + m_\rho} + 4C_7\frac{m_b}{p^2}\left(T_2 + \frac{p^2}{m_B^2 - m_\rho^2}T_3\right),$$

$$B_3 = -C_9^{eff}\frac{2m_\rho}{p^2}(A_3 - A_0) + 4C_7\frac{m_b}{p^2}T_3, \tag{22}$$

$$C_1 = C_{10}\frac{V}{m_B + m_\rho},$$

$$D_1 = C_{10}(m_B + m_\rho)A_1,$$

$$D_2 = C_{10}\frac{A_2}{m_B + m_\rho},$$

$$D_3 = C_{10}\frac{2m_\rho}{p^2}(A_3 - A_0).$$

Using Eqs. (20) and (21) and performing summation over final lepton and ρ meson polarization (in the $B \to \rho\,\ell^+\ell^-$ case), we obtained the following results for the double differential decay rates (the masses of the leptons, in our case electron or muon, are neglected):

$$\frac{d\Gamma^{B\to\pi}}{dp^2dz} = \frac{G^2\alpha^2}{2^{11}\pi^5}\frac{|V_{tb}V_{ts}^*|^2\sqrt{\lambda}}{m_B}\lambda m_B^4(1-z^2)\left[\left(|A|^2 + |C|^2\right)\right], \tag{23}$$

$$\frac{d\Gamma^{B\to\rho}}{dp^2dz} = \frac{G^2\alpha^2}{2^{12}\pi^5 m_B}\frac{|V_{tb}V_{td}^*|^2\sqrt{\lambda}}{}\Bigg\{2\lambda m_B^4\left[m_B^2 s(1+z^2)\left(|A_1|^2 + |C_1|^2\right)\right]$$
$$+\frac{1}{2r}\left[m_B^2\left(\lambda(1-z^2)+8rs\right)\left(|B_1|^2 + |D_1|^2\right) - 2\lambda m_B^4(1-r-s)(1-z^2)\right.$$
$$\times\left(Re\,(B_1 B_2^*) + Re\,(D_1 D_2^*)\right)\bigg] + \lambda^2 m_B^6(1-z^2)\frac{1}{2r}\left(|B_2|^2 + |D_2|^2\right)$$
$$+8m_B^4 sz\sqrt{\lambda}\left(Re\,(B_1 C_1^*) + Re\,(A_1 D_1^*)\right)\Bigg\}, \tag{24}$$

where $z = cos\theta$, θ is the angle between the three–momentum of the ℓ^+ lepton and that of the B meson in the center of mass frame of the lepton pair, $\lambda(1, r_M, s) = 1 + r_M^2 + s^2 - 2r_M - 2s - 2r_M s$, $r_M = \frac{m_M^2}{m_B^2}$, and $s = \frac{p^2}{m_B^2}$ ($M = \pi$ or ρ). The CP violating asymmetry

between $B \to M\ell^+\ell^-$ and $\bar{B} \to \bar{M}\ell^+\ell^-$ decays is defined as

$$A_{CP}(p^2) = \frac{\dfrac{d\Gamma}{dp^2} - \dfrac{d\bar{\Gamma}}{dp^2}}{\dfrac{d\Gamma}{dp^2} + \dfrac{d\bar{\Gamma}}{dp^2}} \ . \tag{25}$$

where

$$\frac{d\Gamma}{dp^2} = \frac{d\Gamma\left(\bar{B} \to M\ell^+\ell^-\right)}{dp^2} \qquad \text{and} \qquad \frac{d\bar{\Gamma}}{dp^2} = \frac{d\Gamma\left(B \to \bar{M}\ell^+\ell^-\right)}{dp^2} \ .$$

The differential decay widths $B \to \pi\ell^+\ell^-$ and $B \to \rho\,\ell^+\ell^-$ can easily be obtained from Eqs. (23) and (24) by integrating over z. Finally we get the following results for CP violating asymmetry for the $B \to \pi\ell^+\ell^-$ and $B \to \rho\,\ell^+\ell^-$ decays

$$A_{CP}^{B\to\pi}(p^2) \simeq -\frac{2}{\left(|A|^2 + |C|^2\right)}\Bigg\{ |f_+|^2 \,(\mathrm{Im}\lambda_u)\,(\mathrm{Im}\xi_1^*\xi_2) \tag{26}$$
$$+ \ f_+ f_T \frac{2m_b}{m_B + m_\pi}\Big[\,(\mathrm{Im}\xi_1)\,\eta_2 - (\mathrm{Im}\lambda_u)\,(\mathrm{Im}\xi_2)\,\eta_1 + (\mathrm{Re}\lambda_u)\,(\mathrm{Im}\xi_2)\,\eta_2\Big]\Bigg\} \ ,$$

$$A_{CP}^{B\to\rho}(p^2) \simeq \frac{1}{\Sigma^\rho}\Bigg\{ -2\,(\mathrm{Im}\lambda_u)\,(\mathrm{Im}\xi_1^*\xi_2)\left[\frac{16}{3}\lambda m_B^6 s\left|\frac{V}{m_B + m_\rho}\right|^2 + \frac{2\lambda^2 m_B^6}{3r}\left|\frac{A_2}{m_B + m_\rho}\right|^2\right.$$
$$+ \ \frac{1}{2r}m_B^2\left(\frac{4}{3}\lambda + 16rs\right)(m_B + m_\rho)\,|A_1|^2 - \frac{4}{3}\lambda m_B^4\frac{(1 - r - s)}{r}A_1 A_2\bigg]$$
$$+ \ \Big[2\,(\mathrm{Im}\xi_1)\,\eta_2 - 2\,(\mathrm{Im}\lambda_u)\,(\mathrm{Im}\xi_2)\,\eta_1 + 2\,(\mathrm{Re}\lambda_u)\,(\mathrm{Im}\xi_2)\,\eta_2\Big]$$
$$\times \ \left[\frac{64\lambda m_B^6 m_b s}{3p^2}\frac{T_1 V}{m_B + m_\rho} + \frac{8\lambda^2 m_B^6 m_b}{3rp^2}\frac{A_2}{m_B + m_\rho}\left(T_2 + \frac{p^2}{(m_B^2 - m_\rho^2)}T_3\right)\right.$$
$$+ \ \frac{2m_B^2 m_b}{rp^2}\left(\frac{4}{3}\lambda + 16rs\right)A_1 T_2(m_B + m_\rho)(m_B^2 - m_\rho^2)$$
$$- \ \frac{2}{3}\lambda m_B^4(1 - r - s)\left((m_B + m_\rho)\frac{4m_b}{p^2}A_1\left(T_2 + \frac{p^2}{(m_B^2 - m_\rho^2)}T_3\right)\right.$$
$$+ \ \frac{4m_b(m_B - m_\rho)}{p^2}A_2 T_2\bigg)\bigg]\Bigg\} \ , \tag{27}$$

where

$$\Sigma^\rho = \frac{16}{3}\lambda m_B^6 s\left(|A|^2 + |C|^2\right) + \frac{2}{3r}\lambda^2 m_B^6\left(|B_2|^2 + |D_2|^2\right)$$
$$+ \ \frac{1}{2r}\left[m_B^2\left(\frac{4}{3}\lambda + 16rs\right)\left(|B_1|^2 + |D_1|^2\right)\right.$$
$$- \ \frac{8}{3}\lambda m_B^4(1 - r - s)\Big((\mathrm{Re}B_1 B_2) + (\mathrm{Re}D_1 D_2)\Big)\bigg] \ . \tag{28}$$

In deriving these expressions, we have used the following parametrization

$$
\begin{aligned}
C_9^{eff} &\equiv \xi_1 + \lambda_u \xi_2 \ , \\
C_7^{eff} &\equiv \eta_1 + i\,\eta_2 \ ,
\end{aligned}
\tag{29}
$$

and assumed that all form factors are positive (see below). Interference of C_9^{eff} and C_7^{eff} terms gives new contribution to the CP violating asymmetry. The results for the CP asymmetry in model II can be obtained from Eqs. (26) and (27) by substituting Eq. (3) (i.e., $\eta_2 = 0$).

At the end of this section we present forward–backward asymmetry A_{FB}, which involve different combination of the Wilson coefficients. The analysis of A_{FB} is very useful in extracting precise information about the sign of the Wilson coefficients and the new physics. The forward–backward asymmetry is defined as

$$
A_{FB}(p^2) = \frac{\displaystyle\int_0^1 dz \frac{d\Gamma}{dp^2 dz} - \int_{-1}^0 dz \frac{d\Gamma}{dp^2 dz}}{\displaystyle\int_0^1 dz \frac{d\Gamma}{dp^2 dz} + \int_{-1}^0 dz \frac{d\Gamma}{dp^2 dz}} \ .
\tag{30}
$$

The forward–backward asymmetry for the $B \to \pi \ell^+ \ell^-$ decay is zero, both in SM and 2HDM, in the limit $m_\ell \to 0$. We can explain this fact briefly as follows. The hadronic current for $B \to \pi \ell^+ \ell^-$ decay is a pure vector and the lepton current is also conserved when $m_\ell \to 0$. The charge asymmetry (or A_{FB}) is non–zero if there exist C–viloating terms but such terms are clearly absent in the $B \to \pi \ell^+ \ell^-$. Using Eq. (24), the forward–backward asymmetry for the $B \to \rho\, \ell^+ \ell^-$ takes the following form:

$$
A_{FB}^\rho = \frac{8m_B^4 s \sqrt{\lambda}\Big[(\mathrm{Re}B_1 C_1^*) + (\mathrm{Re}A_1 D_1^*) \Big]}{\Sigma^\rho} \ .
\tag{31}
$$

Finally, we examine the CP–violating difference between A_{FB} and $\bar{A}_{FB}$, i.e.,

$$
\delta A_{FB} = A_{FB} - \bar{A}_{FB} \ ,
$$

with $\bar{A}_{FB}$ being the forward–backward asymmetry in the anti particle channel, which can be obtained by the replacement

$$
C_9^{eff}(\lambda_u) \to \bar{C}_9^{eff}(\lambda_u \to \lambda_u^*) \ ,
$$

whose explicit can easily be obtained from Eq. (31), with the above mentioned replacement of C_9^{eff}.

4   Numerical analysis

Before presentation of our quantitative calculations and graphics, we would like to note that we have considered two different versions, namely model II and model III of the 2HDM, in our analysis. For the free parameters λ_{bb} and λ_{tt} of model III, we have used the restrictions

coming from $B \to X_s \gamma$ decay, B^0–$\bar{B}^0$ mixing, ρ parameter and neutron electric–dipole moment [28], that yields $|\lambda_{bb}| = 50$, $|\lambda_{tt}| \leq 0.03$.

The values of the main input parameters, which appear in the expressions for the branching ratios, A_{FB} and A_{CP} are: $m_b = 4.8 \; GeV$, $m_c = 1.4 \; GeV$, $m_\tau = 1.78 \; GeV$, $m_B = 5.28 \; GeV$, $m_\pi = 0.14 \; GeV$. For B meson lifetime we take $\tau(B) = 1.56^{-12} \; s$ [36]. The values of the Wilson coefficients are, $C_1 = -0.249$, $C_2 = 1.108$, $C_3 = 1.112 \times 10^{-2}$, $C_4 = -2.569 \times 10^{-2}$, $C_5 = 7.4 \times 10^{-3}$, $C_6 = -3.144 \times 10^{-2}$. Throughout the course of the numerical analysis, we have used the Wolfenstein parametrization of the CKM matrix elements, i.e.,

$$\lambda_u = \frac{V_{ub}V_{ud}^*}{V_{tb}V_{td}^*} = \frac{\rho(1-\rho) - \eta^2 + i\,\eta}{(1-\rho)^2 + \eta^2} + \mathcal{O}(\lambda^2) \,,$$

for which we have used the following three different sets of parameters,

$$(\rho, \eta) = \begin{cases} (0.3; 0.34) \\ (-0.07; 0.34) \\ (-0.3; 0.34) \,. \end{cases}$$

Of course the explicit expressions for the form factors are needed in the present numerical analysis. In the current literature these form factors have been calculated in the framework of the three point QCD sum rule [37], relativistic quark model [38], and light cone QCD sum rules [39–41]. In further numerical analysis we have used the light cone QCD sum rule predictions on the form factors. It should be noted that the light cone QCD sum rule predictions on the form factors are reliable in the region $m_b^2 - p^2 \sim \mathcal{O}(\text{few } GeV^2)$. In order to extend to the full physical region we have used best fitted expressions by extrapolating the numerical results with the condition that these approximate formulas reproduce the light cone QCD sum rule predictions to a good accuracy, in the above–mentioned region. The form of form factors which satisfy this condition can be written in terms of three parameters as [39, 40]

$$F(p^2) = \frac{F(0)}{1 - a_F \dfrac{p^2}{m_B^2} + b_F \left(\dfrac{p^2}{m_B^2}\right)^2} \,,$$

where the values of parameters $F(0)$, a_F and b_F for the relevant decays, $B \to \pi$ and $B \to \rho$, are listed in Table 1 (this Table is taken from [39, 40]

Firstly we consider model II for numerical calculations. In Figs. (1) and (2) we present the dependence of the differential decay widths of the $B \to \pi e^+ e^-$ and $B \to \rho e^+ e^-$ on p^2 for $(\rho, \eta) = (0.3; 0.34)$ at $m_{H^\pm} = 250 \; GeV$ and $tan\beta = 1$, with and without long distance contributions, correspondingly. In Figs. (3) and (4) we plot the variation of the CP–violating asymmetry A_{CP} with respect to p^2, with the following set of parameters: $(\rho, \eta) = (0.3; 0.34)$ and $tan\beta = 1$. In both figures, the solid line corresponds to the SM case, dash–dotted and dotted lines represent the CP–violating asymmetry at two different values of the mass of charged Higgs boson $m_{H^\pm} = 250 \; GeV$ and $500 \; GeV$, respectively. The total branching ratios for the $B \to \pi e^+ e^-$ and $(B \to \rho e^+ e^-)$ decays at three different sets

of Wolfenstein parameters and at $m_{H^\pm} = 250\ GeV$ are presented in Table 2. From Figs. 1–4 we see that, in model II the dependences of the branching ratio and A_{CP} asymmetry on p^2 are very similar to those predicted by the SM, but their magnitudes different in these models. These results are expected, since in model II, the charged Higgs contributions change only the values of the Wilson coefficients C_7, C_9 and C_{10}. In this version of the 2HDM charged Higgs contributions give rise to constructive interference to the SM result. Therefore the branching ratio increases and CP asymmetry decreases.

We presented in Table 2, the numerical values of the average values of the CP violating asymmetry $\langle A_{CP} \rangle$, in the region $1\ GeV^2 < p^2 < \left(m_{J/\psi} - 0.02\ GeV \right)^2$, using the same values of the Wolfenstein parameters used in Figs. 3 and 4.

The dependence of the forward–backward asymmetry on p^2 $A_{FB}(B \to \rho\, e^+ e^-)$ is plotted in Fig. (5) for SM and model II, with the same set of parameters as in Fig. (1). It is observed that the value of p^2 at which A_{FB} becomes zero is shifted in model II. Therefore, in future experiments, the determination of the value of p^2 at which A_{FB} is zero can give unambiguous information about the presence of new physics. In Fig. (6) we plot the resulting difference in the forward–backward asymmetry for the values of Wolfenstein parameters $(\rho, \eta) = (-0.07; 0.2)$, with and without the long distance effects. From these figures we observe that, δF_{AB} for the $B \to \rho\, e^+ e^-$ decay is positive in the non resonant region for all values of p^2, both in SM and model II.

Note that, the results we have presented for forward–backward asymmetry and its difference are performed for $(\rho, \eta) = (-0.07; 0.2)$. However, for sake of completeness, we have gone through the same analysis for two different sets of the Wolfenstein parameters, namely, $(\rho, \eta) = (-0.3; 0.34)$ and $(\rho, \eta) = (-0.07; 0.34)$, as well as several different choices of $\tan\beta$. The numerical results and the relevant graphical presentations have demonstrated that, no remarkable differences have been observed among these different choices. In Figs. (7) and (8) we present the dependence of the CP asymmetry A_{CP}, integrated over p^2, for the $B \to \pi e^+ e^-$ and $B \to \rho\, e^+ e^-$ decays on the phase angle θ at $m_{H^\pm} = 250\ GeV$, $|\lambda_{bb}| = 50$ and $|\lambda_{tt}| = 0.03$, without the long distance effects in model III. From both figures, especially from $B \to \rho\, e^+ e^-$ case, we observe that, the average CP asymmetry differs essentially from the one predicted by model II. In the region $\pi/2 < \theta < 3\pi/2$, the change in $\langle A_{CP} \rangle$ is more than 2.5 times than that predicted by model II. This fact can be explained as, the charged Higgs and SM contributions interference destructively in the above–mentioned region of θ. It should be stressed that, depending on the value of the phase angle θ, the charged Higgs contributions can interfere with the SM results, either constructively or destructively. This case is absolutely different in model II, where the above–mentioned contributions interfere only constructively. The values of the branching ratios $B \to \pi \ell^+ \ell^-$ and $B \to \rho\, \ell^+ \ell^-$ decays at different values of the phase angle θ in model III are presented in Table 4.

In conclusion, the exclusive $B \to \pi \ell^+ \ell^-$ and $B \to \rho\, \ell^+ \ell^-$ decays are analyzed in the 2HDM and it is found that, the CP violating asymmetry in model III differs essentially from the ones predicted by model II.

References

[1] J. L. Hewett, In *Stanford 1993, Proceedings, Spin structure in high energy processes* 463-475 (1993).

[2] W. S. Hou, R. S. Willey and A. Soni, Phys. Rev. Lett. **58**, 1608 (1987).

[3] N. G. Deshpande and J. Trampetic, Phys. Rev. Lett. **60**, 2583 (1988).

[4] C. S. Lim, T. Morozumi and A. I. Sanda, Phys. Lett. B **218**, 343 (1989).

[5] B. Grinstein, M. J. Savage and M. B. Wise, Nucl. Phys. B **319**, 271 (1989).

[6] C. Dominguez, N. Paver and Riazuddin, Phys. Lett. B **214**, 459 (1988).

[7] N. G. Deshpande, J. Trampetic and K. Ponose, Phys. Rev. D **39**, 1461 (1989).

[8] P. J. O'Donnell and H. K. Tung, Phys. Rev. D **43**, 2067 (1991).

[9] N. Paver and Riazuddin, Phys. Rev. D **45**, 978 (1992).

[10] A. Ali, T. Mannel and T. Morozumi, Phys. Lett. B **273**, 505 (1991).

[11] A. Ali, G. F. Giudice and T. Mannel, Z. Phys. C **67**, 417 (1995).

[12] C. Greub, A. Ioannissian and D. Wyler, Phys. Lett. B **346**, 145 (1995);
D. Liu, Phys. Lett. B **346**, 355 (1995);
G. Burdman, Phys. Rev. D **52**, 6400 (1995);
Y. Okada, Y. Shimizu and M. Tanaka, Phys.Lett. B **405**, 297 (1997).

[13] A. J. Buras and M. Münz, Phys. Rev. D **52**, 186 (1995).

[14] N. G. Deshpande, X. -G. He and J. Trampetic, Phys. Lett. B **367**, 362 (1996).

[15] S. Bertolini, F. Borzumati, A. Masiero, G. Ridolfi,
Nucl.Phys. B **353**, 591 (1991).

[16] F. Krüger and L. M. Sehgal Phys. Rev D **55**,2799 (1997).

[17] F. Krüger and L. M. Sehgal Phys. Rev D **56**, 5452 (1997).

[18] S. Glashow and S. Weinberg, Phys. Rev D **15**, 1958 (1977).

[19] Talk by R. Briere, CLEO-CONF-98-17, ICHEP98-1011, in Proceedings of ICHEP98, Vancouver, Canada, July 1998; and in talk by J. Alexander, in Proceedings of ICHEP98, Vancouver, Canada, July 1998.

[20] R. Barate *et al.*, ALEPH Collaboration, Phys. Lett. B **429**, 169 (1998).

[21] F. Borzumati and C. Greub, Phys. Rev D **58**, 074004 (1998).

[22] M. Ciuchini, G. Degrassi, P. Gambino, G.F. Giudice, Nucl.Phys B **527**, 21 (1998).

[23] K. Kiers and A. Soni, Phys. Rev D **56**, 5786 (1997).

[24] A. Stahl, H. Voss, Z. Phys C **74**, 73 (1997).

[25] T.P. Cheng and M. Sher, Phys. Rev D **35**, 3484 (1987); *ibid.* D **44**, 1461 (1991);
W.S. Hou, Phys. Lett. B **296**, 179 (1992);
A. Antaramian, L. Hall, and A. Rasin, Phys. Rev. Lett **69**, 1871 (1992);
L. Hall and S. Weinberg, Phys. Rev D **48**, 979 (1993);
M.J. Savage, Phys. Lett B **266**, 135 (1991).

[26] D. Atwood, L. Reina, and A. Soni, Phys. Rev D **55**, 3156 (1997).

[27] L. Wolfenstein and Y.L. Wu, Phys. Rev. Lett **73**, 2809 (1994).

[28] D. Bowser-Chao, K. Cheung, W.-Y. Keung, hep–ph/9811235 (1998).

[29] G. Buchalla, A. Buras, and M. Lautenbacher, Rev. Mod. Phys **68**, 1125 (1996).

[30] A.J. Buras, M. Misiak, Münz, and S. Pokorski, Nucl. Phys B **424**, 374 (1994).

[31] B. Grinstein, R. Springer, and M. Wise, Nucl. Phys B **339**, 269 (1990).

[32] M. Misiak, Nucl. Phys B**393**, 23 (1993), Erratum, *ibid.* B **439**, 461 (1995);
A. J. Buras and M. Münz, Phys. Rev D **52**, 186 (1995).

[33] A. I. Vainshtein, V. I. Zakharov, L. B. Okun and M. A. Shifman,
Sov. J. Nucl. Phys **24**, 427 (1976).

[34] F. Jegerlehner, Nucl.Phys.Proc.Suppl **51C**, 131 (1996).

[35] T. Kinoshita, B. Nižić and Y. Okamata, Phys. Rev D **31**, 2108 (1985).

[36] Particle Data Group, R. M. Barnett *et al.*, Phys. Rev D **54**, 1 (1996).

[37] P. Colangelo, F. De Fazio, P. Santorelli and E. Scrimieri,
Phys. Rev D **53**, 3672 (1996).

[38] W. Jaus and D. Wyler, Phys. Rev D **41**, 3405 (1990);
D. Melikhov, N. Nikitin and S. Simula, Phys.Lett B **410**, 290 (1997).

[39] P. Ball, J.High Energy Phys 9809:005 (1998).

[40] P. Ball, V. M. Braun, Phys.Rev D **58**, 094016 (1998).

[41] T. M. Aliev, A. Özpineci and M. Savcı, Phys. Rev D **56**, 4260 (1997).

Figure captions

Fig. 1 Invariant mass squared (p^2) distribution of the branching ratio of the electron pair in the $B \to \pi e^+ e^-$ decay. Line 1 corresponds to the mass spectrum including the effects of ρ, ω and J/Ψ resonances, whereas line 2 corresponds to the non resonant invariant mass spectrum, in the SM. Analogously, lines 3 and 4 represents the same distributions, respectively, in the model II, at $tan\beta = 1$. In both models the Wolfenstein parameters are chosen to be $(\rho, \eta) = (0.3, 0.34)$.

Fig. 2 The same as in Fig. 1, but for the $B \to \rho e^+ e^-$ decay.

Fig. 3 CP–violating partial width asymmetry in the $B \to \pi e^+ e^-$ decay as a function of p^2 for the values of the Wolfenstein parameters $(\rho, \eta) = (0.3, 0.34)$, including ρ, ω and J/Ψ resonances. Line 1 represents the SM. Lines 2 and 3 correspond to the model II case for the different choices of the charged Higgs boson mass $m_H^{\pm} = 500\,GeV$, and $m_H^{\pm} = 250\,GeV$, respectively.

Fig. 4 The same as in Fig. 3, but for the $B \to \rho e^+ e^-$ decay.

Fig. 5 The dependence of the forward–backward asymmetry A_{FB} on p^2 in the $B \to \rho e^+ e^-$ decay. The Wolfenstein parameters are chosen to be $(\rho, \eta) = (-0.07, 0.2)$. See Fig. 1 for the interpretation of the lines 1 to 4.

Fig. 6 The CP–violating partial width asymmetry difference. $\delta_{FB} = A_{FB} - \bar{A}_{FB}$ in the $B \to \rho e^+ e^-$ decay for $(\rho, \eta) = (-0.07, 0.2)$. See Fig. 1 for the interpretation of the lines 1 to 4.

Fig. 7 The dependence of the CP violating asymmetry, integrated over p^2, on the phase angle θ for the $B \to \pi e^+ e^-$ decay, in model III. In this figure the straight line corresponds to model II. The Wolfenstein parameters and the charged Higgs are chosen to be $(\rho, \eta) = (0.3, 0.34)$ and $m_H^{\pm} = 250\,GeV$, respectively.

Fig. 8 The same as in Fig. 7, but for the $B \to \rho e^+ e^-$ decay.

$10^8 \times \frac{d\mathcal{B}}{dp^2}(B \to \pi e^+ e^-)$

$p^2 \ \left(GeV^2\right)$

THDM

SM

Figure 1:

$10^8 \times \frac{d\mathcal{B}}{dp^2}(B \to \rho e^+ e^-)$

$p^2 \ \left(GeV^2\right)$

THDM

SM

Figure 2:

16

Figure 3:

Figure 4:

17
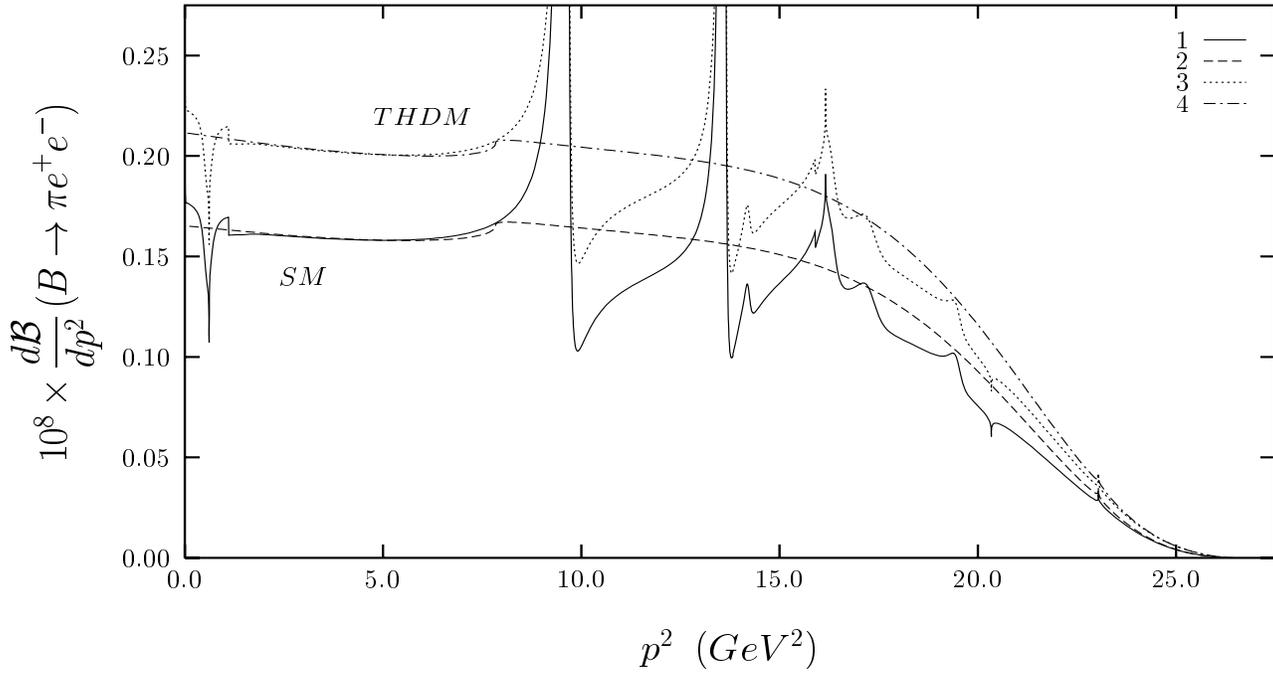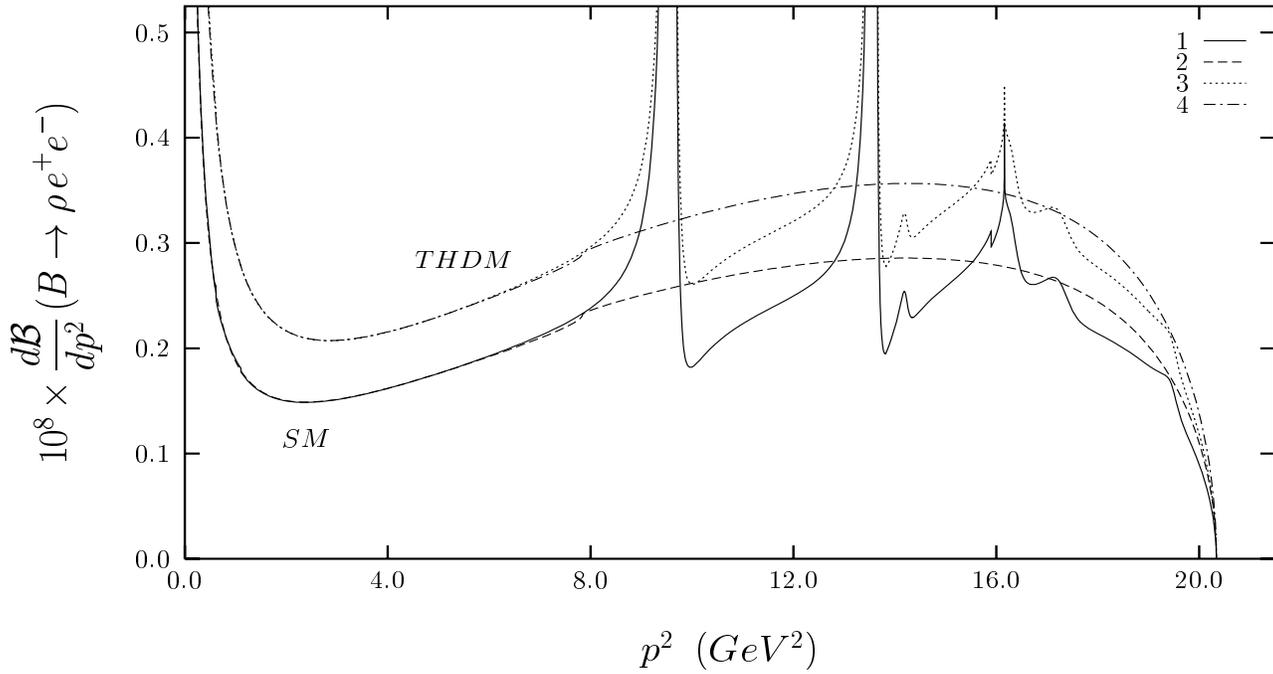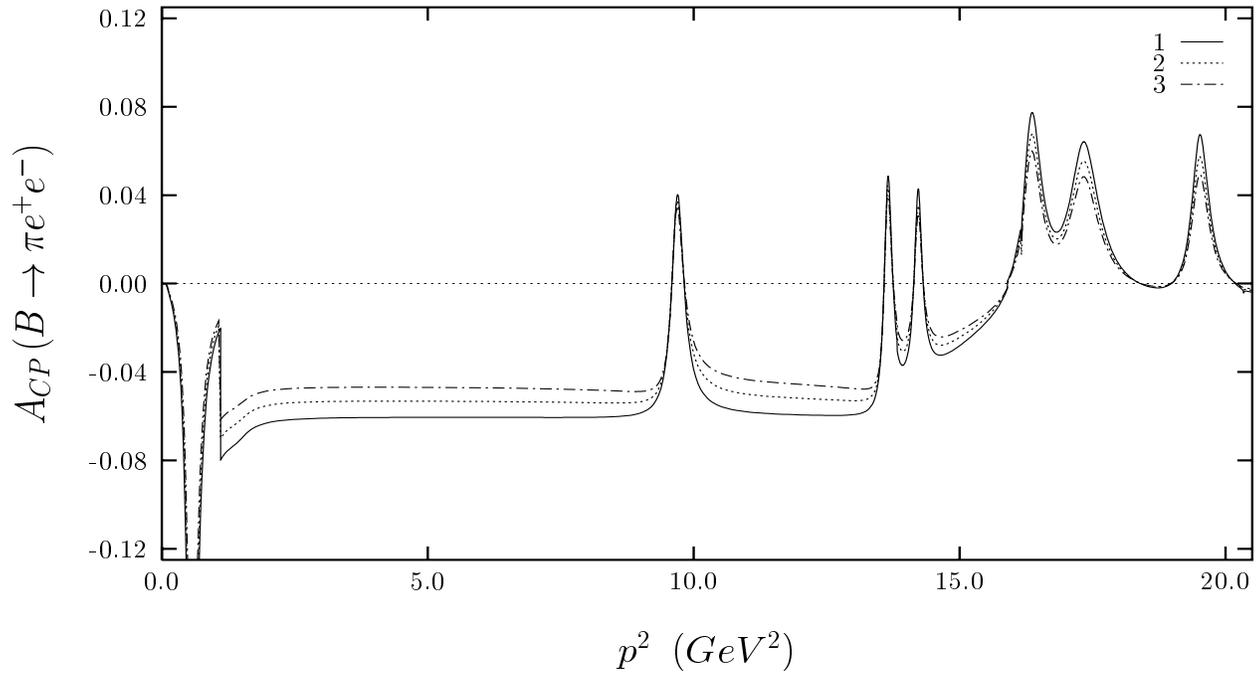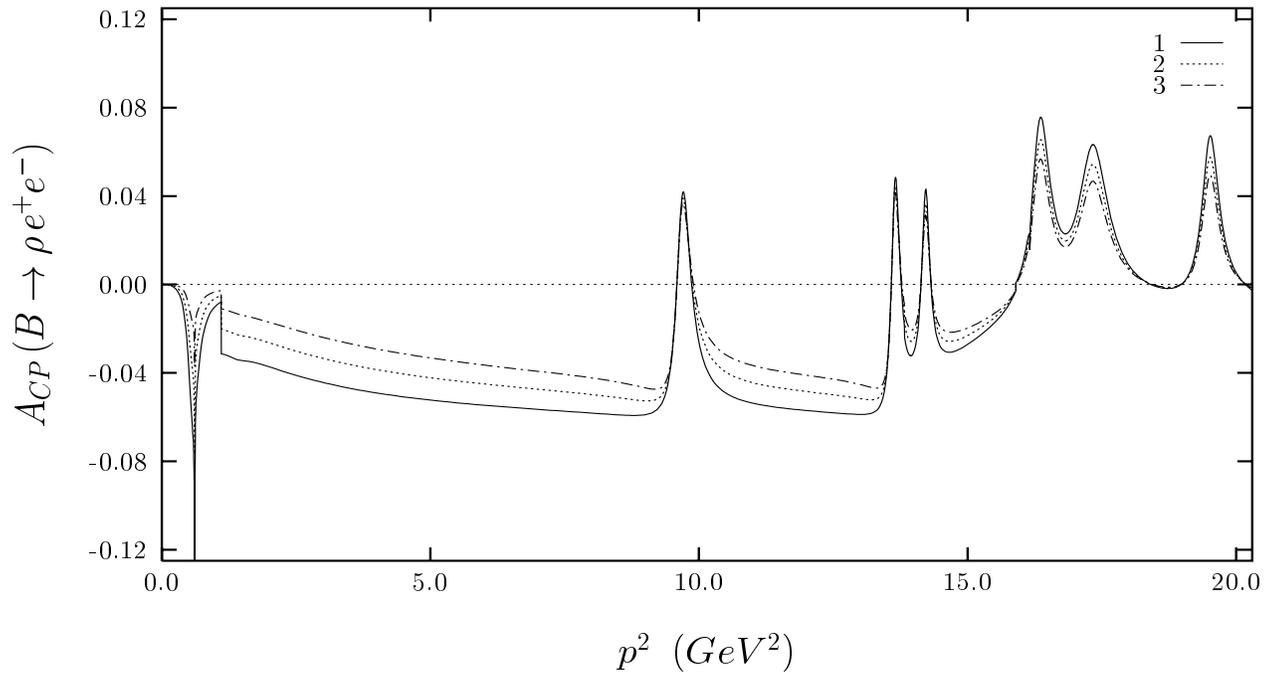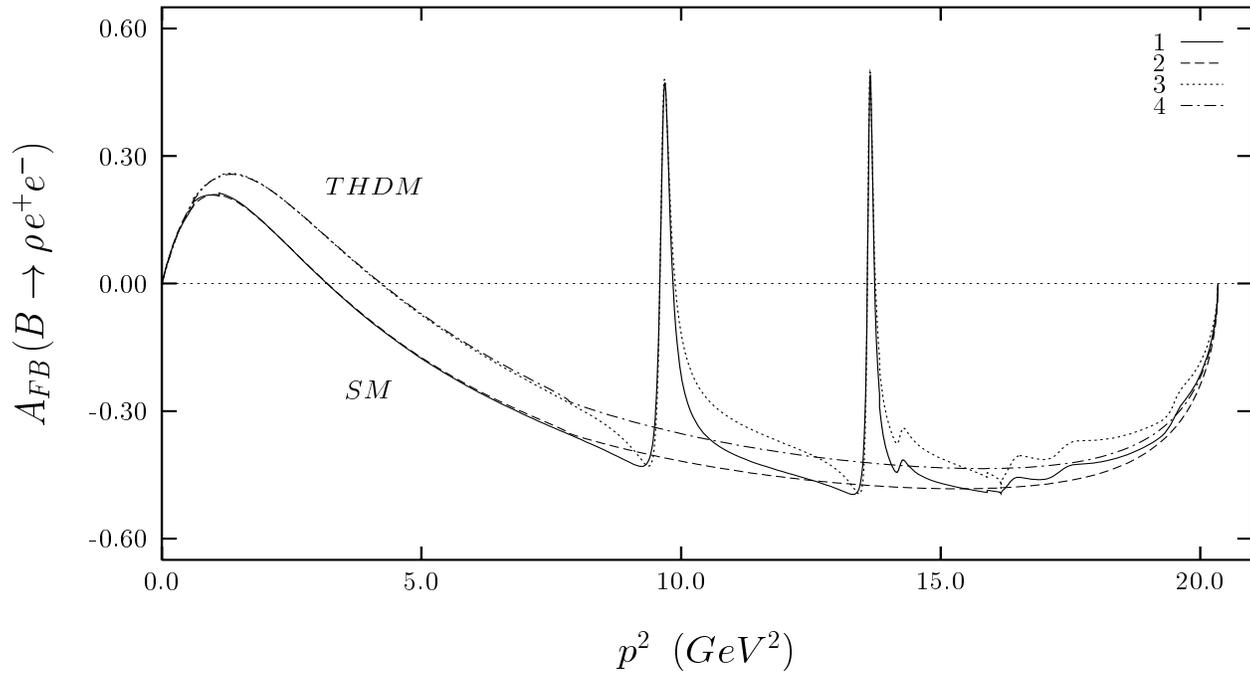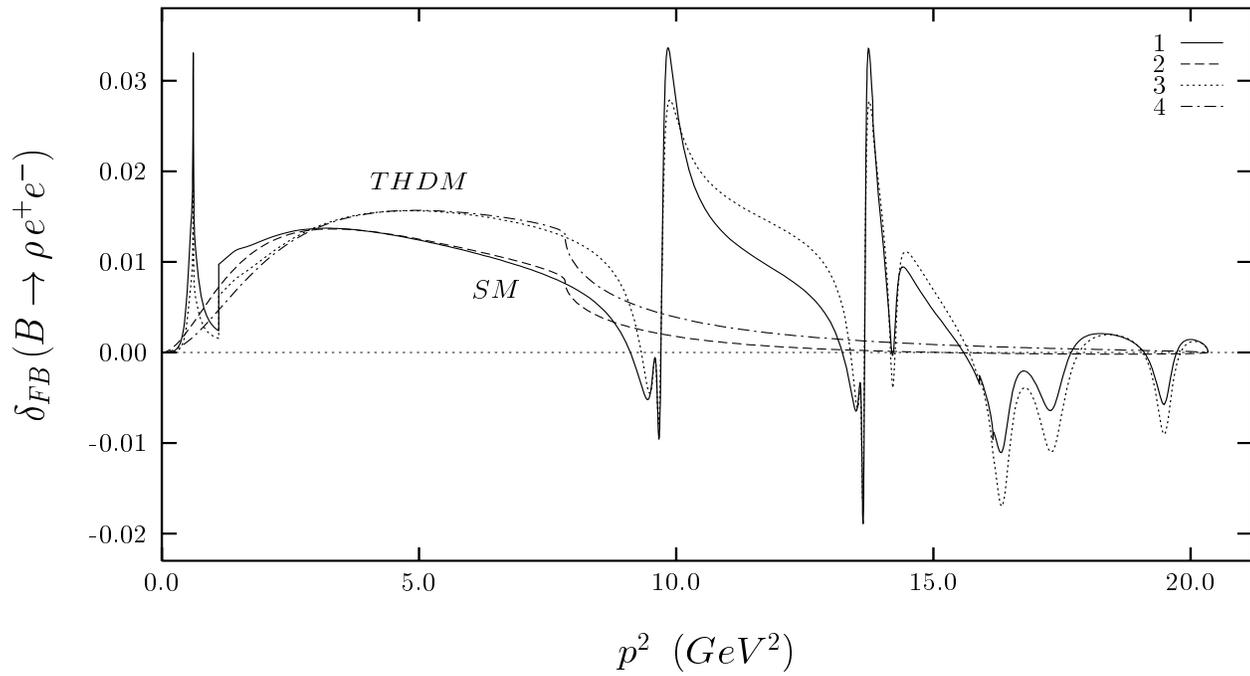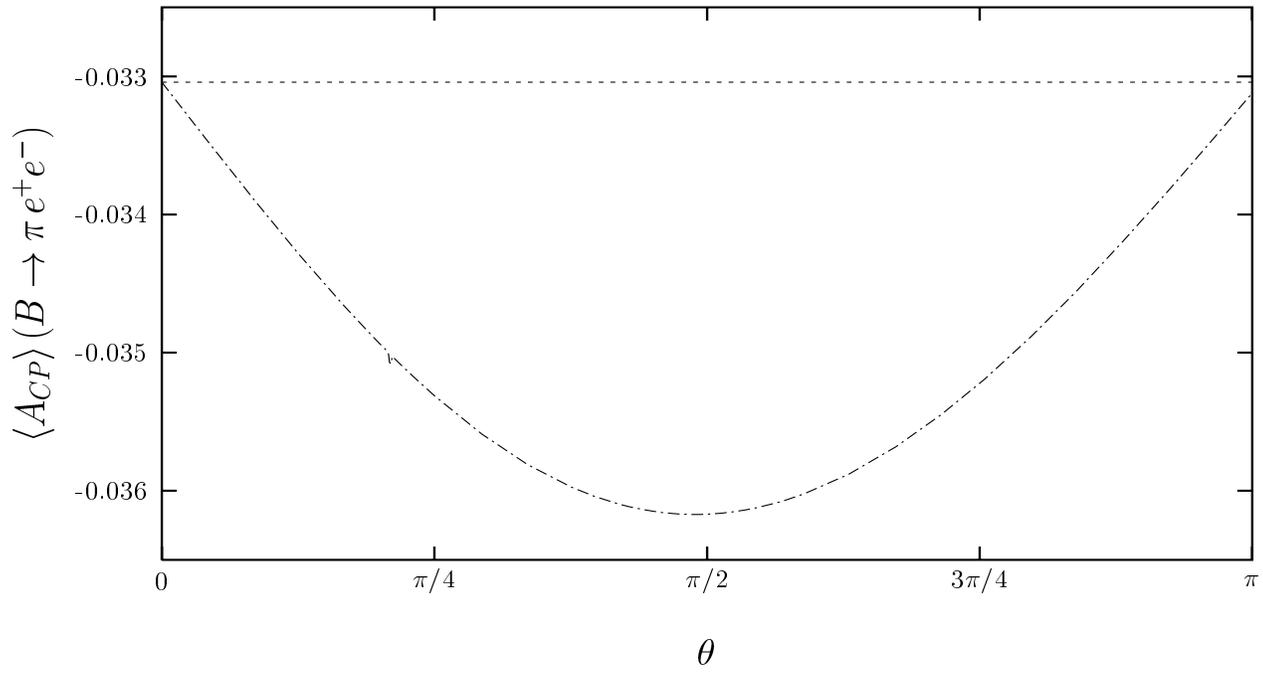
Figure 5:

Figure 6:

Figure 7:
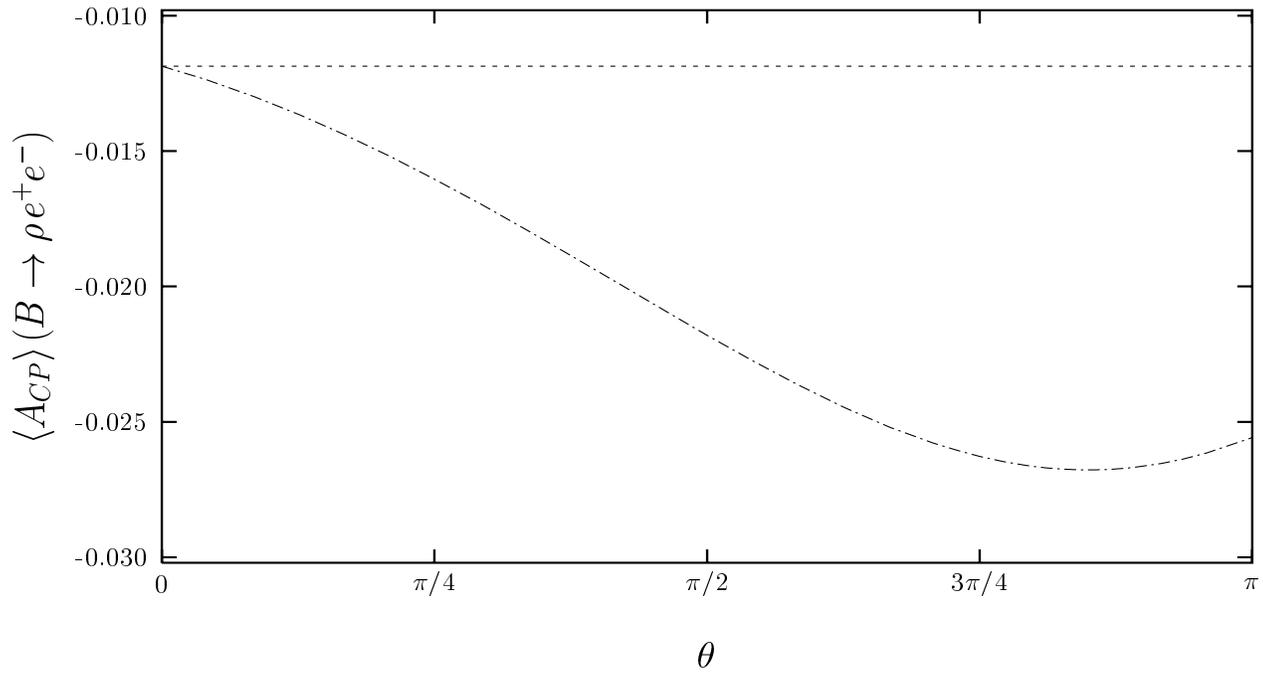
Figure 8:

	$F(0)$	a_F	b_F
$A_1^{B \to \rho}$	0.26 ± 0.04	0.29	-0.415
$A_2^{B \to \rho}$	0.22 ± 0.03	0.93	-0.092
$V^{B \to \rho}$	0.34 ± 0.05	1.37	0.315
$T_1^{B \to \rho}$	0.15 ± 0.02	1.41	0.361
$T_2^{B \to \rho}$	0.15 ± 0.02	0.28	-0.500
$T_3^{B \to \rho}$	0.10 ± 0.02	1.06	-0.076
$f_+^{B \to \pi}$	0.30 ± 0.04	1.35	0.270
$f_T^{B \to \pi}$	-0.30 ± 0.04	1.34	0.260

Table 1:

$(\rho; \ \eta)$	$\mathcal{B}(B \to \pi e^+ e^-)$		$\mathcal{B}(B \to \rho \, e^+ e^-)$	
	SM	THDM	SM	THDM
(+0.3; 0.34)	3.27×10^{-8}	4.11×10^{-8}	5.99×10^{-8}	8.45×10^{-8}
(-0.3; 0.34)	3.31×10^{-8}	4.15×10^{-8}	6.00×10^{-8}	8.46×10^{-8}
(-0.07; 0.34)	3.30×10^{-8}	4.14×10^{-8}	6.00×10^{-8}	8.46×10^{-8}

Table 2:

	$\langle A_{CP} \rangle^{(B \to \pi)}$	$\langle A_{CP} \rangle^{(B \to \rho)}$
$m_{H^\pm} = 250\ GeV$	-0.048	-0.030
$m_{H^\pm} = 500\ GeV$	-0.054	-0.031

Table 3:

θ	$\mathcal{B}(B \to \pi e^+ e^-)$	$\mathcal{B}(B \to \rho\, e^+ e^-)$
0	3.12×10^{-8}	7.41×10^{-8}
$\pi/4$	3.16×10^{-8}	7.08×10^{-8}
$\pi/2$	3.26×10^{-8}	6.34×10^{-8}

Table 4: